The preprophase band is a localized center of clathrin-mediated endocytosis in late prophase cells of the onion cotyledon epidermis

Ichirou Karahara[1], Jinsuke Suda[1,†], Hiroshi Tahara[2,‡], Etsuo Yokota[2], Teruo Shimmen[2], Kazuyo Misaki[3], Shigenobu Yonemura[3], Lucas Andrew Staehelin[4] and Yoshinobu Mineyuki[5,6,*,§]

[1]*Department of Biology, Graduate School of Science and Engineering, University of Toyama, Toyama 930-8555, Japan,*

[2]*Department of Life Science, Graduate School of Life Science, University of Hyogo, 3-2-1 Kouto, Akou, Hyogo 678-1297, Japan,*

[3]*RIKEN Center for Developmental Biology, 2-2-3 Minatojima-minamimachi, Chuou-ku, Kobe 650-0047, Japan,*

[4]*MCD Biology, University of Colorado, Boulder, CO 80309-0347, USA,*

[5]*Department of Biological Science, Hiroshima University, Higashi-Hiroshima 739-8526, and*

[6]*Department of Life Science, Graduate School of Life Science, University of Hyogo, 2167 Shosha, Himeji, Hyogo 671-2280, Japan*

Summary

The preprophase band (PPB) marks the site on the plant cell cortex where the cell plate will fuse during the final stage of cytokinesis. Recent studies have shown that several cytoskeletal proteins are depleted at the PPB site, but the processes that bring about these changes are still unknown. We have investigated the membrane systems associated with the PPB regions of epidermal cells of onion cotyledons by means of serial thin sections and electron tomograms. In contrast with specimens preserved by chemical fixatives, our high-pressure frozen cells demonstrated the presence of large numbers of clathrin-coated pits and vesicles in the PPB regions. The vesicles were of two types: clathrin-coated and structurally related, non-coated vesicles. Quantitative analysis of the data revealed that the number of clathrin-coated pits and vesicles is higher in the PPB regions than outside of these regions. Immunofluorescent microscopy using anti-plant clathrin-antibody confirmed this result. In contrast, no differences in secretory activities were observed. We postulate that the removal of membrane proteins by endocytosis plays a role in the formation of PPB 'memory' structures.

Keywords: preprophase band of microtubules, endocytosis, electron tomography, clathrin-coated pits, clathrin-coated vesicles.

Introduction

Orientation of cell division is an essential factor for morphogenesis and development in higher plants (Sinnott, 1960). Some genes like *TANGLED1* (Smith *et al.*, 1996) have been shown to be involved in the control of the division pattern, but their molecular mechanism has yet to be determined. The preprophase band (PPB) of microtubules (MTs), which underlies the plasma membrane, delineates the future site of cell plate fusion with the mother cell plasma membrane, and it has been postulated to be involved in the determination of the site of cell division (Mineyuki, 1999;

Pickett-Heaps and Northcote, 1966a,b). The PPB originates during the G2 phase as a broad band of MTs that narrows to reach its most compact state during the late prophase (Mineyuki *et al.*, 1988). Upon completion, the narrow PPB is disassembled, and its tubulin subunits are recycled into spindle MTs during the prometaphase (Wick and Duniec, 1983; Wick *et al.*, 1981). Because the cell plate, which is assembled in the telophase, fuses with the plasma membrane at the site defined by the narrow PPB, it has been postulated that the PPB leaves behind information or

'memory' in some yet unidentified form at or in the plasma membrane (Mineyuki and Gunning, 1990).

The process of PPB narrowing seems to be functionally important (Mineyuki and Palevitz, 1990). After the narrowing of the PPB MTs, cortical actin, which is typically distributed uniformly under the plasma membrane, becomes depleted in the PPB zone (Baluška et al., 1997; Cleary, 1995; Cleary et al., 1992; Liu and Palevitz, 1992). The kinesin-like molecule KCA1 has also been shown to be depleted in this zone (Vanstraelen et al., 2006). The finding that the actin- and the KCA1-depleted zones persist long after PPB breakdown, has led to the suggestion that the narrowed PPB leaves behind a 'negative memory' that affects the anchoring of actin and KCA1 to the plasma membrane. Evidence for a 'positive memory' has also been obtained. The *tangled* (*tan*) gene product co-localizes with the PPB, and remains there after the PPB MTs disappear (Walker et al., 2007). Mineyuki and Gunning (1990) have shown that the cortical division site marked by the PPB contains a factor that solidifies the nascent cell plate. A microtubule-associated protein, AIR9 (Buschmann et al., 2006), and TPLATE, a protein with a domain similar to that of vesicular coat proteins (Van Damme et al., 2006), accumulate at the former PPB site when the cell cortex is contacted by the outwardly growing cytokinetic apparatus.

How these memory sites are created is still unknown. A long-standing hypothesis is that marking of the PPB zone involves local changes in plasma membrane composition. This hypothesis originated from studies of PPB formation in chemically-fixed cells, which demonstrated the presence of electron-dense vesicles in the PPB region (Burgess and Northcote, 1968; Galatis and Mitrakos, 1979; Gunning et al., 1978; Packard and Stack, 1976). It was noted that the vesicles resembled cell walls in their staining properties (Packard and Stack, 1976), that they stained with periodate acid-thiocar-bohydrazide silver proteinate, a polysaccharide stain (Galatis, 1982), and that in some Leguminosae, wall thickenings develop at the site of the PPB (Galatis et al., 1982). These observations led to the suggestion that the creation of the PPB memory site could involve deposition of memory-forming molecules by secretion. However, the presence of similar vesicles underlying non-PPB regions raised early doubts about the idea that secretion deposits positive markers at the PPB site (Galatis, 1982; Galatis and Mitrakos, 1979). Furthermore, as shown by Dixit and Cyr (2002), inhibition of Golgi secretion by brefeldin A during PPB formation has no effect on cell plate fusion at the PPB site in tobacco BY-2 cells.

Although a direct role of clathrin in plant endocytosis has yet to be demonstrated experimentally, the paradigm for clathrin-coated vesicles selectively removing membrane proteins is well documented in animal and fungal systems (Bonifacino and Traub, 2003; Kirchhausen, 2000), and the uptake of specific molecules by means of endocytosis has been observed in plants (Gifford et al., 2005; Kim et al., 2006; Russinova et al., 2004; Shah et al., 2002). Several electron microscopical studies on PPBs have reported the presence of vesicles in the cytoplasm underlying the PPB, but only in guard mother cells of legumes have coated vesicles been observed (Galatis and Mitrakos, 1979; Galatis et al., 1982). The combination of high-pressure freezing and electron tomography techniques has enabled us to analyze the distribution of the clathrin-coated pits and vesicles quanti-tatively. To test whether the rate of endocytosis is enhanced in PPB regions, we have quantified the distribution of clathrin-coated pits and vesicles, as well as of secretory structures, during PPB formation in high-pressure frozen meristem cells of onion cotyledons, both in serial thin sections and in electron tomograms. Our results provide support for the idea that modification of the cell cortex at PPB sites involves endocytosis in the PPB-associated plasma membrane domains.

Results

We used epidermal cells of 3-day-old onion cotyledons for analyses of membrane structures in PPBs, because PPB development in this cell type is well characterized (Mineyuki et al., 1989). In the basal region of 3-day-old onion cotyle-dons, ~3% of the cells are undergoing mitosis at any one time. Late prophase cells with a narrow PPB can be distin-guished from interphase cells, based on the characteristic staining pattern of the condensed chromosomes (Figure 1; Nogami et al., 1996). Because most of the divisions are anticlinal and symmetrical, it is possible to cut sections with the PPBs in a predetermined orientation. We have exploited this feature to obtain quantitative information on the secre-tory and endocytic structures associated with the outer and inner walls of PPB-forming epidermal cells.

Clathrin-coated pits are readily discerned in PPBs of high-pressure frozen cells

As illustrated in Figure 2a, b, the electron microscopical observation of tangential thin sections of cryofixed/freeze-substituted onion epidermal cells showed exceptionally clear images of clathrin-coated pits and MTs in PPBs. The quality of our sample preparation can be seen from the fact that in many instances we could distinguish the hexagon and pentagon lattice elements of the clathrin coats. To identify late prophase cells with narrow PPBs, we first observed the mid longitudinal section of each cell, to view the nucleus, and only then progressed to the preparation of tangential sections of the PPB region. The use of electron tomography has enabled us to identify, map and model the pits, vesicles and MTs of PPB regions with a much higher degree of resolution than is possible with thin sections (Figures 3a, b and 4). Quantitative analysis of the distribution
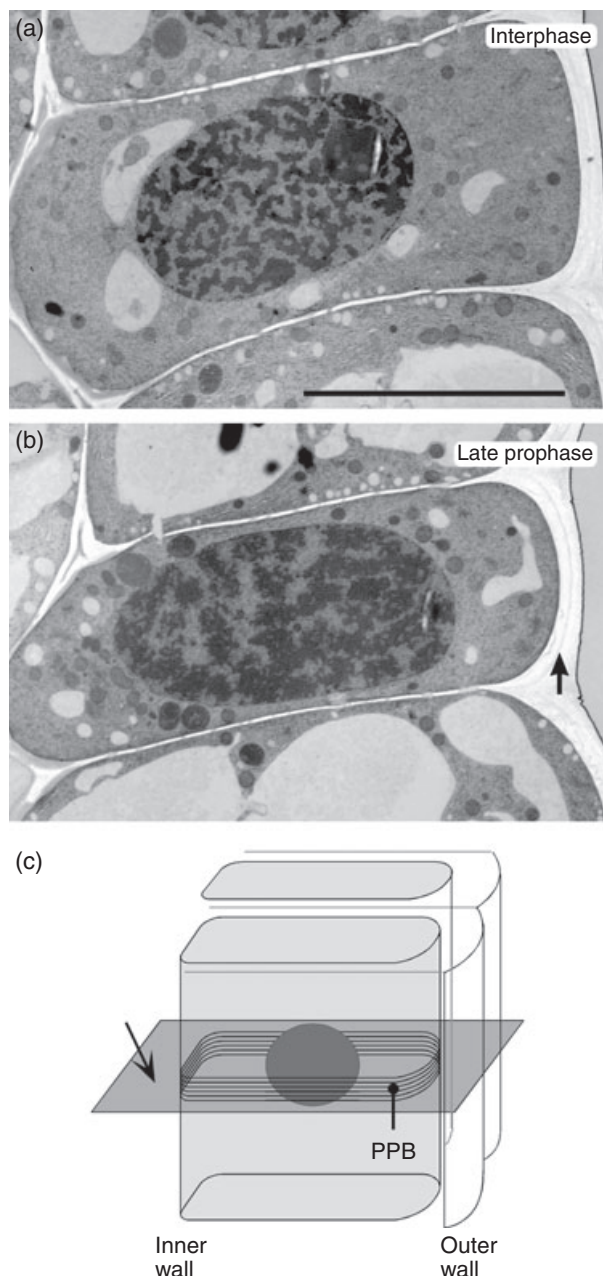
Figure 1. Electron micrographs of cross-sections through epidermal cells of an onion cotyledon at the level of the nucleus.
(a) Interphase cell. Scale bar: 10 μm.
(b) Late prophase cell, as identified by the condensed chromatin. Arrow: outer wall.
(c) Schematic illustration depicting the plane of the sections (arrow).

of the clathrin-coated pits at the cortical region closest to the nucleus of late prophase and interphase cells showed that the average frequency of coated pit occurrence was the same, ∼4 μm^{-2}, in both types of cells. In contrast, the comparison of the average frequency of clathrin-coated pit occurrence between the PPB (nuclear) and the non-PPB

(extranuclear) regions of the plasma membrane clearly showed that the frequency of the occurrence of clathrin-coated pits was reduced in the non-PPB domains (Table 1).

PPB formation is accompanied by a decrease in the number of clathrin-coated vesicles outside of the PPB region

The specimen preparation protocol employed in this study in onion epidermal cells was optimized for the staining of the MTs, and of the clathrin-coated pits and vesicles. Of particular value for this study was the fact that it also produced a characteristic, high-contrast staining of the molecules bound to the clathrin-coated pits, and of the contents of the vesicles (Figures 2a, b, 3 and 5). Although the staining pattern within the pits varied slightly, the stain density was so high that the pits could be easily discerned against the background (Figure 2b). As illustrated in Figures 2c, d, 3 and 5, the same dark staining pattern is evident in thin sections and tomographic slice images of clathrin-coated vesicles (Figure 5a), and in vesicles with no coats (Figure 5d). Although most vesicles in the cell cortex examined in the tomographic images were either dark-core, clathrin-coated vesicles (Figure 5a) or dark-core, non-coated vesicles (Figure 5d), we did observe some dark-core vesicles with partial coats (Figures 5b, c). This suggests that the dark-core, non-coated vesicles could be derived from the dark-core, clathrin-coated vesicles.

The average frequencies of occurrence of dark-core, clathrin-coated and non-coated vesicles in the cytoplasm underlying the external wall at the nuclear (PPB) and extranuclear (non-PPB) levels of late prophase cells, and those at the nuclear level of interphase cells, are summarized in Table 1. These results show that in late prophase cells the frequency of the occurrence of clathrin-coated vesicles is notably lower in the region outside of the PPB than in the PPB region. On the other hand, the frequency of the occurrence of the dark-core, clathrin-coated vesicles in the PPB region of late prophase cells was twofold higher than in the interphase cells. Furthermore, the frequency of the occurrence of dense-core, non-coated vesicles in late prophase cells was increased more than threefold compared with interphase cells.

The frequency of the occurrence of clathrin-containing cytoplasmic structures revealed by immunofluorescent microscopy is highest in and around the PPBs

To confirm that clathrin molecules are present in the PPB, we localized clathrin in interphase and prophase cells of onion epidermal cells by immunofluorescent microscopy. The anti-clathrin heavy-chain antibodies used in this experiment (Tahara *et al.*, 2007) cross-reacted with a single band at 175 kDa in immunoblot extracts from onion seedlings (Figure S1). This antibody cross-reacted with two types of
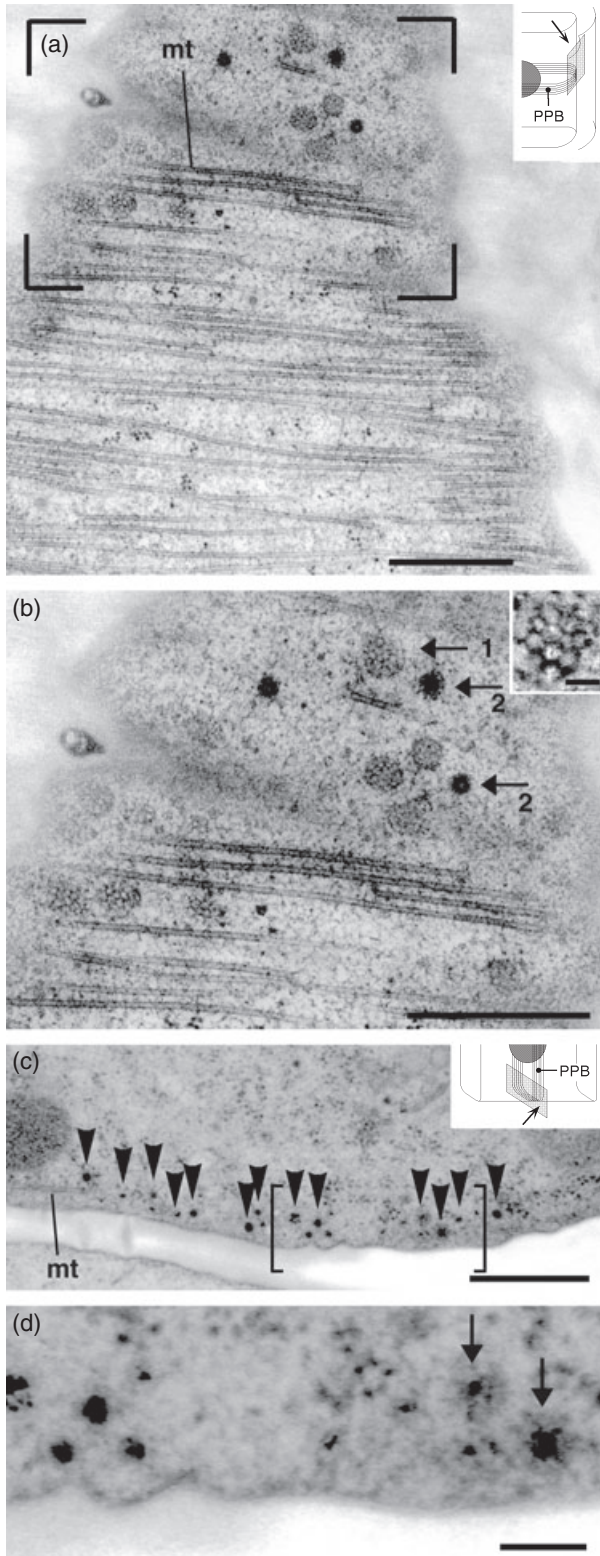
Figure 2. Electron micrographs of thin-sectioned epidermal cells showing clathrin-coated pits, vesicles and microtubules (MTs) in the preprophase band (PPB) region.

(a) Overview of a tangential section through the outer cell wall and adjacent cytoplasm. The majority of the PPB MTs appear to be closely aligned. Abbreviations: mt, MT; PPB, PPB region. An illustration in the upper right corner shows the location of the section in a cell (indicated with an arrow). Scale bar: 0.5 μm.

(b) Detail of the bracketed region shown in (a). Clathrin-coated pits are seen in the PPB. Although there are no MTs seen in the upper half of this region in this image, MTs were presumed in this cytoplasmic domain in the adjacent thin section: 1, shallow clathrin-coated pit displaying a typical clathrin lattice; 2, clathrin-coated pits associated with forming vesicles with darkly stained bound internal molecules. Inset: 7.1-nm-thick, composite tomographic slice image, illustrating the hexagon and pentagon lattice elements of the clathrin coats. Scale bars: 1 μm (inset, 50 nm).

(c) Overview micrograph of a cross section through the inner wall and adjacent cytoplasm (see inset diagram), illustrating cortical vesicles and a PPB MT. Many vesicles can be seen just beneath the plasma membrane (arrowheads); mt, MT. An illustration in the upper right corner shows the location of the section in a cell (indicated with an arrow). Scale bar: 0.5 μm.

(d) Detail of the cortical vesicles in the region marked by the brackets in (c). Some, but not all, vesicles appear to be surrounded by a coat (indicated with arrows). Scale bar: 0.2 μm.

throughout the cytoplasm, whereas the small, dim structures were seen mostly in the cell cortex, both in interphase (Figure 6a, b, 6cl, dl) and in prophase cells (Figure 6c, d). These results suggest that the small, dim fluorescent structures seen in the confocal images correspond to the clathrin-coated pits and vesicles seen in the cell cortex of thin-sectioned cells (Figures 2, 3 and 4).

These confocal micrographs not only confirm the presence of clathrin-containing structures in the PPBs, but also provide an independent means for characterizing the distribution of clathrin pits and vesicles in prophase and interphase cells. In interphase cells, clathrin-coated pits and vesicles are distributed evenly on the cell surface (Figure 6a), whereas in late prophase cells they are more abundant in the PPB region (Figure 6c). Comparison of the frequency of occurrence of the anti-clathrin-stained dim fluorescent dots observed in PPBs (at the nuclear level in late prophase cells), and in non-PPB cortical regions (at the extranuclear level in late prophase and interphase cells), of immunofluorescence photographs (Table S1) also confirmed that the frequency of the occurrence of clathrin-containing dim fluorescent dots is higher in the PPB regions, than in the other regions. However, because the number of clathrin-containing dim fluorescent dots per square micron was smaller than the number of clathrin-coated pits and vesicles determined by electron tomography, one fluorescent dot may correspondent to a cluster of several clathrin-coated pits and vesicles. In addition, Figure 6c demonstrates that in prophase cells the region containing higher frequencies of occurence of clathrin-coated pits and vesicles extends beyond the edge of the bundled PPB MTs. Together, these fluorescence microscopy results confirm the distribution of clathrin-coated pits and vesicles, as determined by the electron tomographic studies (Figure 4b).

intracellular structures in the onion epidermal cells (Figure 6): large, brightly stained objects, and small, dim structures. The brightly stained objects were distributed
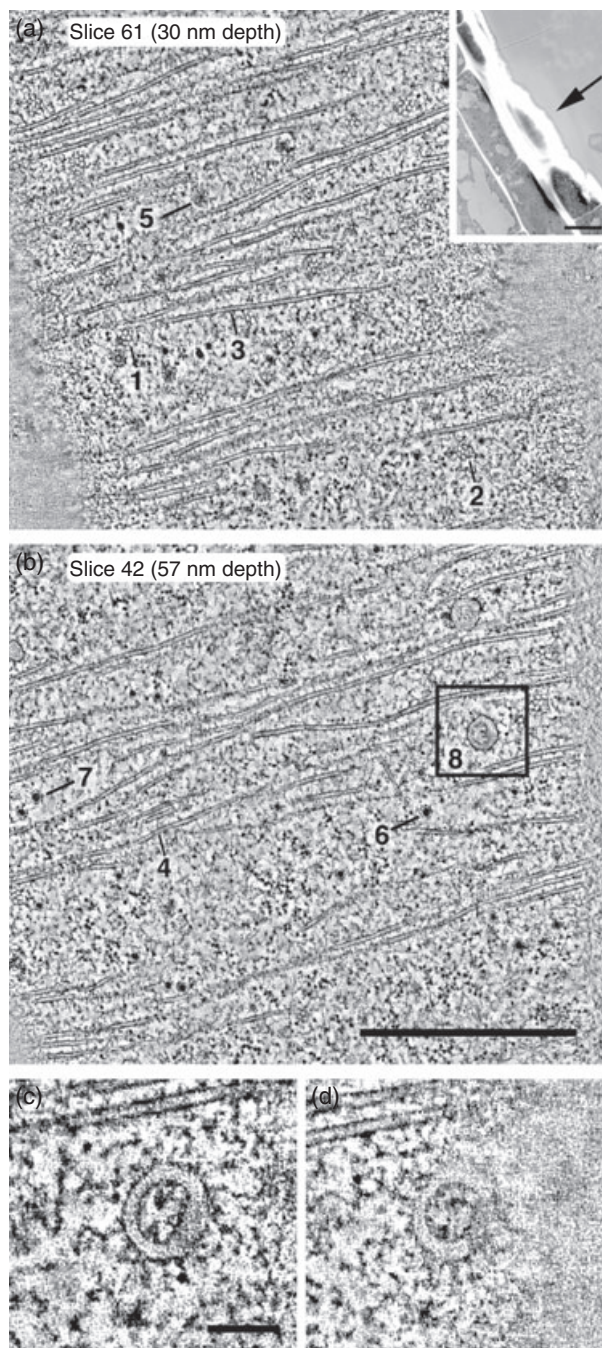
Figure 3. Tomographic images of a tangentially sectioned preprophase band (PPB) in a late prophase epidermal cell. The tomogram contained a total of 110 slices, with the higher slice numbers showing areas closer to the plasma membrane. Structures: 1 and 2, mature, vesicle-shaped, clathrin-coated pits; 3 and 4, two microtubules (MTs); 5, a detached clathrin-coated vesicle; 6, clathrin lattice of a shallow clathrin-coated pit; 7, non-coated vesicle; 8, horseshoe-shaped plasma membrane infoldings.
(a, b) Two images of 1.42-nm-thick tomographic slices. Inset: overview electron micrograph of the 250-nm section used to make the tomogram. Scale bars: 1 μm (inset, 10 μm).
(c, d) Higher magnification tomographic slice images of horseshoe-shaped plasma membrane infoldings, shown in the black rectangle in (b): (c) (slice 54) and (d) (slice 60) are different sections through the same horseshoe structure framed in (b). Scale bar: 0.1 μm.

The frequency of endocytic vesicle occurrence in the cell cortex underlying the inner and outer cell wall domains is the same

As illustrated in Figure 1a, b, the outer walls of epidermal cells are considerably thicker than the inner walls. In addition, the outer walls are covered by a cuticle. To determine whether the vesicle distribution in the cortical cytoplasm underlying the inner and outer cell wall regions was the same, we measured the frequency of the occurrence of all vesicles with dark cores in serial thin sections of cells sectioned in the plane of their PPBs (Figure 7; Table 2). These measurements demonstrated that the highest frequency of vesicle occurrence was found within a 400-nm-wide zone of cytoplasm underlying the plasma membrane (Figure 8). The same set of micrographs also enabled us to determine the average frequency of cortical vesicle occurrences in PPB and non-PPB regions, as well as compare the frequency of vesicle occurrences underlying the outer and inner walls of the same cells. However, because of the lower magnification of the electron micrographs used for making the whole-cell montages, we were unable to positively identify all of the clathrin-coated vesicles (see Figure 2d). For this reason, Table 2 only refers to cortical vesicles with dark cores, but does not distinguish between clathrin-coated and non-coated vesicles. The frequency of dark-core vesicle occurrence at the nuclear level was higher in PPB-containing cells than in interphase cells. No differences were seen in the extranuclear levels. We also found no differences in the frequency of the occurrence of dark-core vesicles in the cytoplasm underlying the outer versus the inner cell wall regions.

There is no increase in the horseshoe-shaped exocytic structures in the plasma membrane regions associated with PPBs

When a secretory vesicle fuses with the plasma membrane of an animal cell, the plasma membrane expands, and this change in surface area can be readily accommodated by changes in the surface architecture of the plasma membrane. Turgor pressure prevents this from happening in plant cells, because the plasma membrane is tightly pressed against the cell wall, and cannot expand except by forming an infolding. Thus, when a spherical secretory vesicle fuses with the plasma membrane of a turgid plant cell, the vesicle collapses into a disc-shaped membrane appendage that is converted into a characteristic, horseshoe-shaped infolding during membrane recycling (Staehelin and Chapman, 1987). These horseshoe-shaped membrane configurations can be readily identified in cryofixed cells, and are used as a diagnostic tool for quantifying secretory events in a given cell. Two horseshoe-shaped plasma membrane infoldings are illustrated in the tomographic slice images shown in Figure 3c, d. We have quantitatively analyzed the distribution of
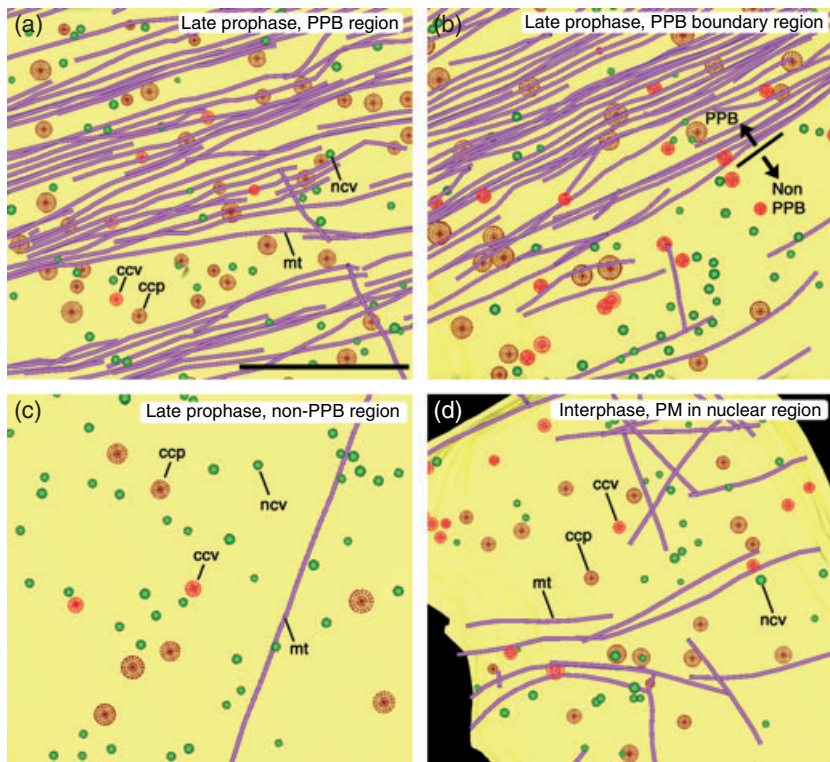
Figure 4. Tomography-based reconstructions of the cortical region at the nuclear level (i.e. preprophase band, PPB, region) (a), at the boundary region between a PPB and a non-PPB region (b), at the extranuclear level (c) of a late prophase, and at the nuclear level of an interphase cell (d). Abbreviations: ccp, clathrin-coated pit (deep red); ccv, clathrin-coated vesicle (bright red); ncv, non-coated vesicle (green); mt, MT (purple); pm, plasma membrane (yellow). Scale bar: 1 μm.

Table 1 Average frequency of the occurrence of clathrin-coated pits and vesicles, and non-coated vesicles at the nuclear (preprophase band, PPB, region) and extranuclear (non-PPB region) level of late prophase, and at the nuclear level of interphase cells (non-PPB region)

	Interphase	Late prophase	
	Nuclear (non-PPB)	Nuclear (PPB region)	Extranuclear (non-PPB)
Clathrin-coated pits[A]	4.0 ± 0.6	4.1 ± 0.5[a]	1.6 ± 0.4*
Clathrin-coated vesicles[B]	13.4 ± 1.7*	26.6 ± 9.9[a]	7.2 ± 0.1**
Non-coated vesicles[A]	25.1 ± 4.1*	87.8 ± 16.5[a]	84.6 ± 15.4

The results are based on measurements made on tomographic data sets. The frequency of the occurrence is expressed as number of pits per μm^2 in the case of clathrin-coated pits, and the number of vesicles per μm^3 in the case of vesicles (mean ± SEM, $n = 4$–6). A multiple comparison test was performed for each row. The frequency of the occurrence of the structures in the PPB ([a]the nuclear region in late prophase cells) was compared with the other regions (**$P < 0.01$; *$P < 0.05$) within each row.
[A]Dunnett's parametric multiple comparison test.
[B]Steel's non-parametric multiple comparisons test.

horseshoe-shaped structures in serial thin-sectioned onion epidermal cells (Table 3). This analysis demonstrated that there was no significant statistical difference between the average frequency of the occurrence of horseshoe-shaped structures in the cell cortex at the nuclear level in the late prophase cells (i.e. the PPB region) and that in the interphase
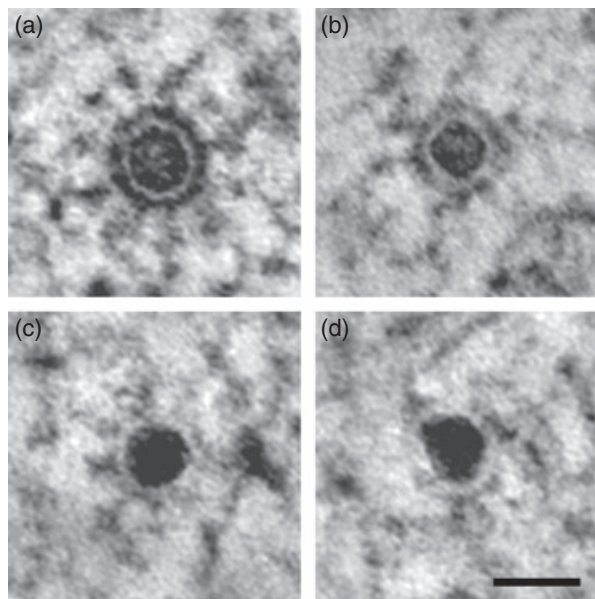

Figure 5. Gallery of 21.3-nm-thick, composite tomographic slice images, illustrating the morphological similarities between clathrin-coated (a), partially coated (b, c) and non-coated (d) dense-core vesicles. Scale bar: 50 nm.

cells. The same result was obtained for the extranuclear-level regions. Together, these findings suggest that formation of the PPB does not affect the rate of vesicle-mediated secretion in the PPB-associated plasma membrane regions.

Figure 6. Distribution of clathrin molecules in high-pressure frozen onion epidermal cells detected by immunofluorescent microscopy. Anti-clathrin labeled structures are colored green, and microtubules are colored red. Panels (a) and (b), and (c) and (d), are the same areas, but (a) and (c) show signals from anti-clathrin, and (b) and (d) show signals of anti-clathrin and anti-tubulin antibodies.

(a, b) Surface of interphase cell. Bracket, nuclear region.

(c, d) Surface of the late prophase cell (P) and the mid-longitudinal plane of the interphase cell (I). Bracket, preprophase band (PPB). Scale bar: 10 μm.
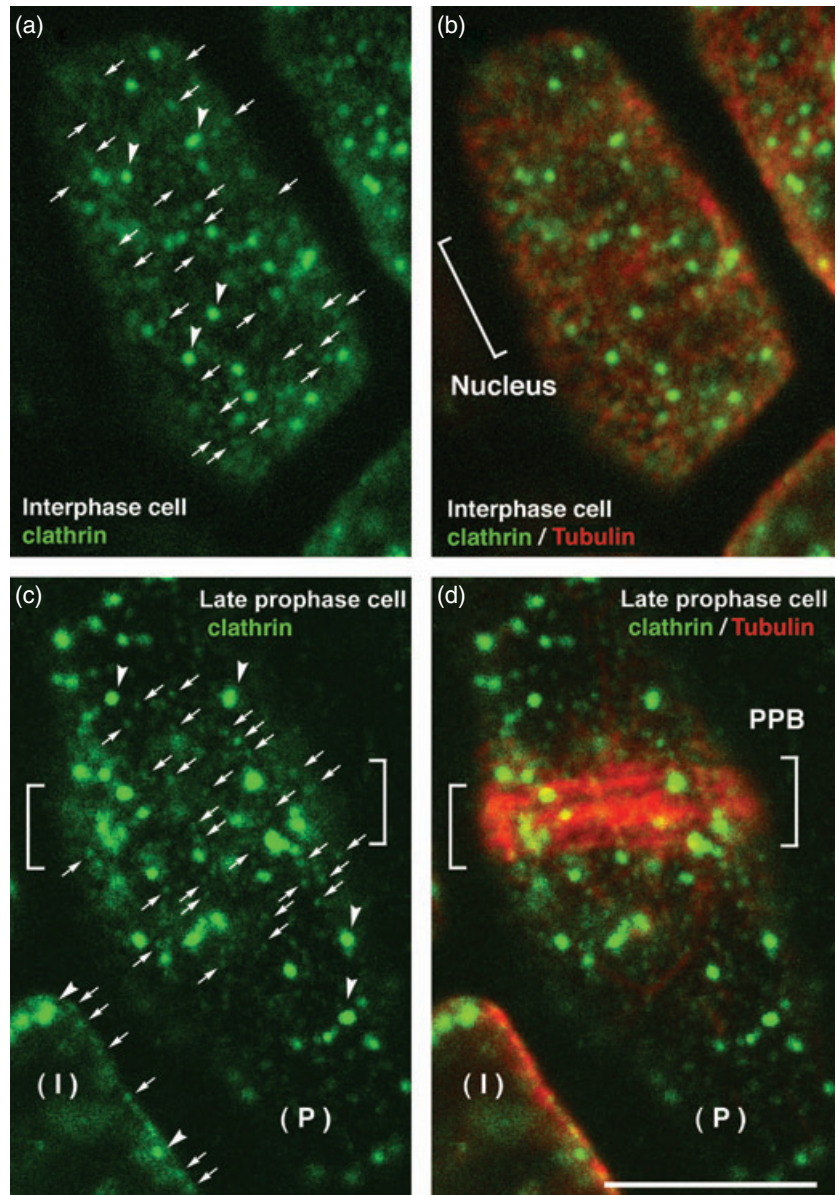
Distribution of Golgi stacks analyzed in serial thin cross sections

Dixit and Cyr (2002) reported that in 10% of their cultured tobacco cells there was a clearly discernable increase in Golgi stack frequency at the PPB site. To determine if onion epidermal cells also accumulate Golgi stacks in the cortical cytoplasm underlying the PPB, we have quantitatively analyzed the distribution of Golgi stacks in our serial thin-sectioned cells to a depth of 400 nm from the plasma membrane (Table 4). This analysis demonstrated that there was no significant statistical difference between the average frequency of Golgi stack occurrence in the cell cortex at the nuclear level in late prophase cells and that in the interphase cells. Similarly, there was no significant statistical difference between the average frequency of Golgi stack occurrence in the cell cortex at the extranuclear level in the late prophase cells and that in the interphase cells. Taken together, these findings demonstrate that there is no marked increase in the frequency of Golgi stack occurrence in the cortical cytoplasm underlying the PPBs in onion epidermal cells.

Discussion

How the PPB marks the future site of cell division has been the subject of many studies and discussions since its discovery in 1966 (Dixit and Cyr, 2002; Gunning and Wick, 1985; Mineyuki, 1999; Pickett-Heaps and Northcote, 1966a,b). The present quantitative characterization of the distribution of both secretory structures and clathrin-coated pits and
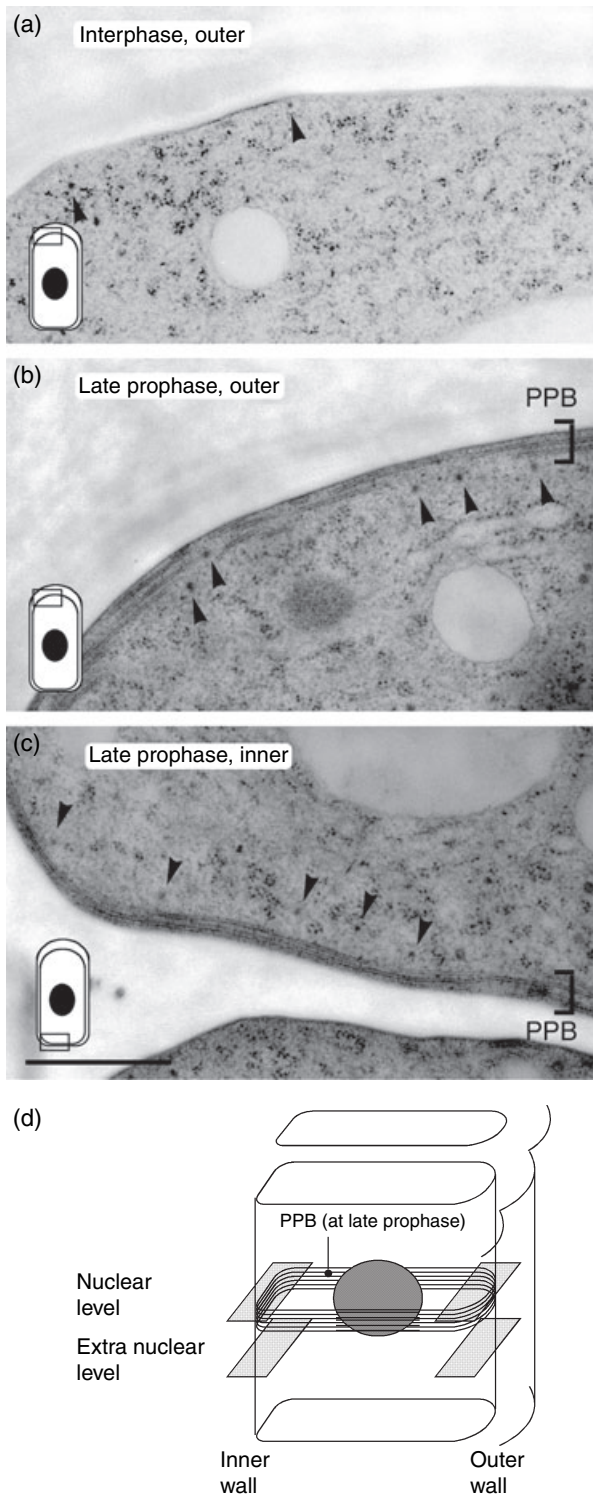
Figure 7. Electron micrographs of thin sections showing the distribution of dark-core vesicles in cortical regions of epidermal cells.
(a) Region beneath the outer cell wall of an interphase cell at the nuclear level.
(b, c) Regions beneath the inner and the outer cell walls of a late prophase cell at the nuclear level, respectively. Note the increase in dark-core vesicles (indicated with arrowheads) in the prophase cell compared with the interphase cell shown in (a). Scale bars: 1 μm.
(d) Schematic illustration depicting the plane of the sections. See also Table 2.

endocytic vesicles in the PPB region of onion epidermal cells, suggests that the reported changes in composition of the plasma membrane of PPB regions could be brought about by the removal of specific plasma membrane molecules from these regions, via clathrin-mediated endocytosis.

PPB regions are centers of enhanced clathrin coated vesicle-mediated endocytosis

Clathrin coated vesicle-mediated endocytosis is an attractive mechanism for locally changing the composition of the plasma membrane at the PPB site, because such vesicles have been shown to concentrate specific types of membrane molecules prior to budding from the donor membrane (Bonifacino and Traub, 2003; Kirchhausen, 2000). Recent studies with the fluorescence marker FM4-64, a purported endocytosis marker, have provided evidence for endocytosis at the PPB (Dhonukshe *et al.*, 2005). However, because FM4-64 may enter cells by mechanisms other than endocytosis (Bolte *et al.*, 2004), the validity of these observations has been questioned. The data produced during the course of the present study demonstrate that the PPB regions are sites of endocytic activity mediated by clathrin-coated vesicles (Figures 2–6). In particular, we demonstrate that the number of clathrin-coated vesicles in the cortical cytoplasm underlying PPB regions increases 3.7-fold compared with non-PPB (extranuclear) regions (Table 1). Furthermore, the increase of the frequency of vesicle occurrence was observed both in the cytoplasm underlying the PPB, adjacent to the thick outer cell wall, and in the thinner inner cell wall of the epidermal cells (Table 2).

Both the electron tomography data (Figure 4b) and the immunofluorescence microscopy results (Figure 6c, d) demonstrate that the region of enhanced endocytosis, mediated by clathrin-coated pits and vesicles, extends beyond the edge of the band of mature PPB MTs. Thus, there seems to be no direct relationship between PPB MTs and the clathrin-coated pits and vesicles involved in endocytosis. This result differs from the findings of the FM4-64 dye uptake study of Dhonukshe *et al.* (2005), in which the uptake of the probe was reported to be confined to the MT-containing PPB region.

Although the MTs in the narrowed PPBs have been thought to be involved in defining the final division site (Mineyuki, 1999; Mineyuki *et al.*, 1989), recent experimental data by Marcus *et al.* (2005) suggests that narrowing of the PPB MTs is not directly involved in producing the signal that is used to guide the cell plate. As Marcus *et al.* (2005) mentioned in their discussion, the new results remind us of the Picket-Heaps' statement (Pickett-Heaps, 1974) that 'the MTs of the PPB look like a weather forecaster that predicts what will happen without taking a direct role in the proceedings'. Thus, the function of the PPB might be to create a planar reference structure and a membrane

Table 2 Average frequency of the occurrence of dark-core vesicles in the preprophase band (PPB) region (inner and outer cortical regions at nuclear level in late prophase cell), and in non-PPB regions (inner and outer cortical regions at extranuclear level in late prophase cell, and inner and outer cortical regions in interphase cell), determined from serially thin cross-sections of onion epidermal cells

Cell stage	Interphase		Late prophase	
Level	Nuclear (non-PPB)	Extranuclear (non-PPB)	Nuclear (PPB region)	Extranuclear (non-PPB)
Outer	14.5 ± 3.1*	10.9 ± 2.8*	36.5 ± 2.4[a]	18.2 ± 3.1*
Inner	10.6 ± 2.2*	17.2 ± 4.4*	36.7 ± 8.4[b]	13.8 ± 2.6*
P (level comparison)	0.40 ($z = 0.84$)	0.40 ($z = -0.84$)	0.40 ($z = 0.84$)	0.53 ($z = 0.63$)

The frequency of the occurrence of dark-core vesicles was compared between the inner and the outer surface of the epidermal cells. The frequency of the occurrence was expressed as numbers of vesicles per μm^3 (mean ± SEM, $n = 5$). The thickness of each section was 70–90 nm. The depth from the plasma membrane analyzed was 400 nm. The plane of the sections is seen in Figure 7d. Steel's non-parametric multiple comparisons test was performed within outer or within inner groups (i.e. within each row). The frequency of vesicle occurrence in the [a]outer region at the nuclear level, or [b]inner region at the nuclear level, in late prophase cells were compared with the other outer regions, or with the other inner regions, respectively (*$P < 0.05$). Furthermore, the Mann–Whitney U-test (two-tailed) was performed between outer and inner regions at each level in each cell stage.
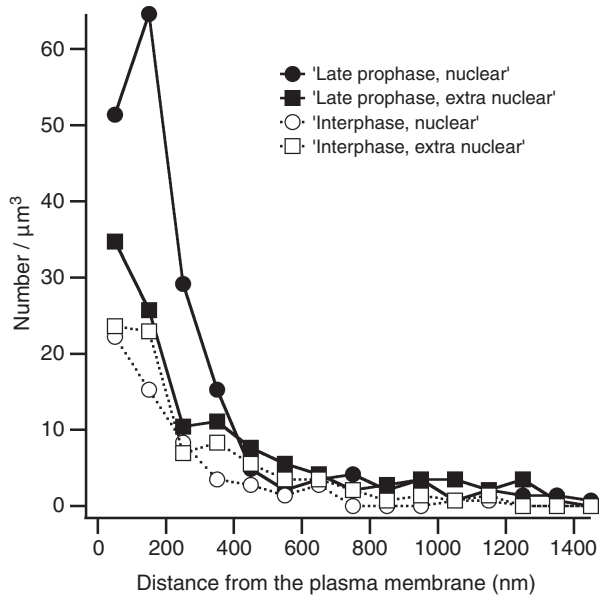

Figure 8. The distribution of dark-core cortical vesicles (clathrin-coated and non-coated) in the depth of the cytoplasm, from the plasma membrane in the preprophase band (PPB) region (inner and outer cortical regions at the nuclear level in the late prophase cell) and non-PPB regions (inner and outer cortical regions at the extranuclear level in the late prophase cell, and inner and outer cortical regions in the interphase cell), as measured in thin cross sections. Each data point represents the mean value of three cells.

environment in which the molecules involved in defining the division site can become organized. The fact that the PPB-associated p34[cdc2] kinase homolog forms a band that is narrower than the PPB (Mineyuki, 1999; Mineyuki *et al.*, 1991) is consistent with this idea. Similarly, the PPB might create a local environment where clathrin-mediated endo-cytosis is stimulated, thereby leading to the desired changes in membrane composition at the future division site.

In plants, endocytosed vesicles have been shown to be transported to multivesicular-type endosomal compart-

Table 3 Average frequency of the occurrence of horseshoe-shaped structures observed in the preprophase band (PPB) region (inner and outer cortical regions at nuclear level in late prophase cell), and in non-PPB cortical regions (inner and outer cortical regions at extranuclear level in late prophase cell, and inner and outer cortical regions in interphase cell), determined from serially thin cross-sections of onion epidermal cells

	Interphase	Late prophase	P (cell stage comparison)
Nuclear level	0.03 ± 0.02	0.15 ± 0.09	0.49 ($z = 0.69$)
Extranuclear level	0.07 ± 0.05	0.27 ± 0.12	0.24 ($z = 1.18$)
P (level comparison)	0.89 ($z = -0.13$)	0.59 ($z = -0.54$)	

The frequency of horseshoe-shaped structures was expressed as numbers of horseshoe-shaped structures per μm^2 (mean ± SEM, $n = 6$). The thickness of each section was 70–90 nm. The Mann–Whitney U-test (two-tailed) was performed at each level.

Table 4 Average frequency of Golgi stack occurrence observed in preprophase band (PPB) region (inner and outer cortical regions at nuclear level in late prophase cell), and in non-PPB cortical regions (inner and outer cortical regions at extranuclear level in late prophase cell, and inner and outer cortical regions in interphase cell), determined from serially thin cross-sections of onion epidermal cells

	Interphase	Late prophase	P (cell stage comparison)
Nuclear level	2.30 ± 0.57	2.04 ± 0.43	0.68 ($z = -0.40$)
Extranuclear level	2.62 ± 0.45	1.47 ± 0.42	0.06 ($z = -1.88$)
P (level comparison)	0.52 ($z = -0.64$)	0.26 ($z = 1.13$)	

The frequency of Golgi stack occurrence was expressed as numbers of stacks per μm^3 (mean ± SEM, $n = 5$). The thickness of each section was 70–90 nm. The depth from the plasma membrane analyzed was 400 nm. The Mann–Whitney U-test (two-tailed) was performed at each level.

ments, where the different components are sorted for recycling or degradation (Jürgens, 2004; Low and Chandra, 1994; Tse *et al.*, 2004). A recent study of apical meristem

cells of *Arabidopsis thaliana* has shown that the onset of clathrin vesicle-mediated endocytosis from cell plates leads to a temporary increase in multivesicular bodies (Seguí-Simarro and Staehelin, 2006). However, in this study of onion epidermal cells we have observed very few multivesicular bodies in the cortical cytoplasm (data not shown), and have been unable to detect any significant increase in multivesicular bodies in the PPB. Thus, we are unable to provide any information on the fate of the endocytosed vesicles.

Secretory activities inside and outside of the PPB region are similar

As a result of the use of cryofixation and freeze-substitution methods, in conjunction with electron tomography, this study has yielded much more reliable and quantifiable information on PPB-related transient membrane events than previous studies of chemically fixed cells. Furthermore, these methodologies provide a means for unambiguously distinguishing between secretory and endocytic events in electron micrographs in plant cells (Staehelin and Chapman, 1987). By quantifying the number of secretory membrane structures (horseshoe-shaped exocytic structures in the plasma membrane), we have demonstrated that the number of secretory events inside and outside of the PPB is essentially the same, and that the number of secretory events is low (Table 3). This strongly suggests that the population of vesicles in the cortical cytoplasm around the PPB region is endocytic, not exocytic. The paucity of PPB-associated secretory structures observed in this study is also consistent with the conclusion of Dixit and Cyr (2002) that Golgi secretion is not required for marking the PPB site.

Endocytosis may help create the 'memory' structures at the PPB

The loss of membrane-bound actin filaments (Baluška *et al.*, 1997; Cleary *et al.*, 1992; Liu and Palevitz, 1992) and kinesin-like protein KCA1 (Vanstraelen *et al.*, 2006) from the PPB site, suggests that formation of the PPB produces local changes in the composition of the plasma membrane. The finding that PPB formation also involves increased rates of endocytosis at the PPB site leads us to consider which types of plasma membrane molecules could be selectively retrieved from this site by means of the clathrin-coated vesicles. One type of candidate protein might be an actin filament-nucleating protein, such as the formin homology (FH) proteins (Banno and Chua, 2000; Favery *et al.*, 2004). Analysis of the genome of *A. thaliana* has led to the identification of 21 genes predicted to be FH proteins (Cvrckova, 2000; Deeks *et al.*, 2002). Several plant formins have the ability to nucleate actin filaments. Overexpression of the group-1 formin AtFH1, an integral plasma membrane protein of

pollen tubes of *A. thaliana*, produces supernumerary actin cables bound to the plasma membrane, tube broadening and growth depolarization (Cheung and Wu, 2004). Similarly, the AtFH6 protein, which has been studied in nematode-induced giant cells, has been found to anchor actin filaments to the plasma membrane of these cells (Favery *et al.*, 2004). Together, these results suggest that one function of the enhanced endocytosis activity at the PPB might be the removal of actin-nucleating/binding proteins from these plasma membrane domains, thereby creating an actin-free zone optimized for fusion with the expanding cell plate.

Experimental procedures

Plant material

Onion (*Allium cepa* L. cv. Highgold Nigou) seeds were sown on pieces of filter paper wetted with 0.05 M sucrose in distilled water, and were grown in the dark for 2 days at 25°C. Seedlings with less than 1-mm-long roots were transferred to pieces of filter paper wetted with 0.1 M sucrose in distilled water, and were cultured further for 1 day.

High-pressure freezing and freeze substitution

Seedlings in which the length between the bending point of the hook to the base was <10 mm were used for specimen preparation, which was carried out according to the method described in Murata *et al.* (2002), with slight modification. Briefly, a basal part of cotyledon, 1–2 mm in length, was cut with a razor blade in 0.1 M sucrose in distilled water, and was immediately loaded in sample holders filled with the same solution, and then frozen using a high-pressure freezer (BAL-TEC HPM 010; Technotrade International Inc., http://www.technotradeinc.com). The high pressure-frozen tissues were transferred to liquid nitrogen for storage. Freeze-substitution was performed in 2% (w/v) OsO_4 in anhydrous acetone at −80°C for 72 h, at −20°C for 24 h, at 4°C for 18 h, and was then incubated in the same 2% (w/v) OsO_4 solution at 40°C, treated with 5% (w/v) uranyl acetate in methanol, and then infiltrated with a graded series of Spurr's resin (Ted Pella, Inc., http://www.tedpella.com). After several acetone rinses, specimens were teased from the holders and infiltrated in Spurr's resin according to the following schedule: 1% (v/v) resin in acetone (12 h); 2, 4, 6, 8, 10% (v/v) resin (2 h each); 12, 25, 50% (v/v) resin (12 h each); 75% (v/v) resin (24 h); 100% (v/v) resin without accelerator (24 h), twice; 100% (v/v) resin with accelerator (24 h), twice; at each concentration. Polymerization was performed at 70°C for 12 h.

Preparation of serial thin sections for vesicle analysis

PPBs appear from G2 to late prophase (Mineyuki *et al.*, 1988). Cross sections of the embedded tissues (400-nm thick) were cut, stained with toluidine blue O [0.1% (w/v) in 1% (w/v) sodium borate solution], and were observed under a light microscope until an epidermal prophase cell was found on the section. The chromosomes appeared highly condensed during late prophase, and scattered during interphase (Figure 1). Once a late prophase cell was found, serial thin cross sections (70–90-nm thick) were cut at the level of the nucleus, mounted on formvar-coated copper

slot grids, stained with 2% (w/v) uranyl acetate in 60% (v/v) methanol and Reynold's lead citrate, and were finally observed under a conventional electron microscope (JEOL 100C or Philips CM-10) to evaluate the quality of the freezing, and to determine if a PPB was present. Once the cell was confirmed to be well preserved, and to have a PPB, additional serial thin sections were cut both in the nuclear and the extranuclear levels of the cell: these were stained and then photographed at 20 000×, to allow for the counting of vesicles. Duplicate counting of vesicles in neighboring serial sections was carefully avoided.

Specimen preparation for electron tomography

Serial 250-nm-thick tangential sections were mounted on formvar-coated copper slot grids, and were stained with 2% uranyl acetate in 60% methanol and Reynold's lead citrate. After the staining, 10- or 15-nm colloidal gold particles were added to both sides of the grid, to be used as fiducial markers to align the series of tilted images. The grids were coated with carbon to enhance stability. The carbon-coated serial sections were examined under an electron microscope, and those shown to contain an outer cortical region of the target prophase cell were processed for electron tomography.

Dual-axis electron tomography

The 250-nm-thick outer tangential sections of outer epidermal cell wall regions were mounted in a tilt–rotate specimen holder, and were observed either using a JEM-1000 high-voltage microscope (JEOL, http://www.jeol.com) operating at 750 kV, or a TF30 intermediate-voltage Tecnai EM (FEI, http://www.fei.com) operating at 300 kV. The images were taken from +60° to −60° at 1.5° intervals about two orthogonal axes, and were collected with a Gatan digital camera (http://www.gatan.com). When a JEM-1000 was used, the images were taken at 12 000×, and were collected with the digital camera that covered an area of 1.4×1.4 μm^2, and had a resolution of 1024×1024 pixels, at a pixel size of 1.42 nm. To record larger areas, four digitized images of adjacent squares were combined into montaged images. When a TF-30 was used, the images were taken at 23 000×, and were collected with the digital camera that covered an area of 2.0×2.0 μm^2, and which had a resolution of 2048×2048 pixels, at a pixel size of 1.0009 nm.

Tomograms were computed for each set of aligned tilts using the R-weighted back-projection algorithm. Tomograms were aligned with each other, and were combined as described previously (Otegui *et al.*, 2001; Seguí-Simarro *et al.*, 2004) in a total reconstructed volume of $2.8 \times 2.8 \times 0.25$ μm^3, in the case of using the JEM-1000, or $2.0 \times 2.0 \times 0.25$ μm^3, in the case of using the TF-30. Tomograms were displayed and analyzed with Imod, the graphics component of the IMOD software package (Kremer *et al.*, 1996).

Quantitative analysis of cortical vesicles and pits in tomograms

The diameter of the vesicles was defined as the outside diameter of the vesicle membrane. The distance between the center of the cortical vesicles and the plasma membrane was calculated as the difference of the Z position of the center of the vesicles and that of the plasma membrane. The plasma membrane surface area was calculated as the mesh surface area of the model. The Z-factor, compression factor, was determined by an analysis of the diameter of MTs as an internal standard.

Immunostaining

High-pressure frozen tissues were freeze-substituted in methanol. Freeze-substitution was performed at −80°C for 72 h, at −20°C for 24 h and at 4°C for 18 h, and then tissues were incubated in PMEG buffer (50 mM PIPES, 5 mM EGTA, 1 mM MgSO$_4$7H$_2$O, 1% glycerol) at 4°C for 30 min. The samples were transferred at 25°C, and were incubated in 20% glycerol at 25°C. The tissues were glued (AronAlpha; Toagosei Co., http://www.toagosei.co.jp/english) to the glass slide, with the epidermis facing the glass surface. After removal of the bulk of the tissue with a razor blade, the remaining tissue was digested for 20 min with a solution containing 1% Cellulase 'Onozuka' RS (Yakult Honsha Co., Ltd., http://www.yakult.co.jp/english), 0.2% Pectolyase Y-23 (Kyowa Chemical Products Co., Ltd., http://www.kyowachemical.co.jp/eng/products.html), 0.4 M mannitol, 0.1% Nonidet P-40, 1% gelatin from cold-water fish skin (Sigma-Aldrich, http://www.sigmaaldrich.com) and a cocktail of protease inhibitors (Complete; Roche Diagnostics, http://www.roche.com/diagnostics). The remaining subepidermal cells were removed with a fine brush so that the layer of epidermal cells could be observed from its inner surface. After washing with distilled water, samples were extracted with methanol at −20°C for 10 min, and were then washed with phosphate-buffered saline (PBS). Samples were incubated in the mixture of antibodies against α-tubulin (mouse monoclonal; Amersham, http://www.amersham.com) and anti-clathrin heavy chain (175-kDa polypeptide; Tahara *et al.*, 2007) for 90 min. Each antibody was diluted 500-fold with PBS supplemented with 1% gelatin. After washing with PBS for 10 min, samples were incubated with a mixture of secondary antibodies, anti-mouse IgG conjugated with Alexa Fluor 594 (Molecular Probes, Invitrogen, http://www.invitrogen.com) and anti-guinea pig IgG conjugated with Alexa Fluor 488 for 90 min. After washing with PBS for 10 min, samples were covered with a solution containing 50% glycerol, 50 mM Tris buffer, pH 9.0, and 1 mg ml^{-1} *p*-phenylenediamine. Hoechst 33258 (1 μm ml^{-1}; Sigma-Aldrich) was included to stain nuclei, and the samples were observed with an LSM 510 laser-scanning microscope (Zeiss, http://www.zeiss.com).

Supporting information

Additional Supporting Information may be found in the online version of this article:

Figure S1. Western blot analysis of protein extracts from onion seedlings using anti-clathrin heavy chain antibodies.
Table S1. Average frequency of the occurrence of the anti-clathrin stained dots observed in the preprophase band (PPB) region (nuclear level in late prophase cells), and in non-PPB cortical regions (extranuclear level in late prophase cells and in interphase

cells), determined from immunofluorescence micrographs of onion epidermal cells.

Please note: Wiley-Blackwell are not responsible for the content or functionality of any supporting materials supplied by the authors. Any queries (other than missing material) should be directed to the corresponding author for the article.

References

Baluška, F., Vitha, S., Barlow, P.W. and Volkmann, D. (1997) Rearrangement of F-actin arrays in growing cells of intact maize root apex tissues: a major developmental switch occurs in the post-mitotic transition region. *Eur. J. Cell Biol.* **72**, 113–121.

Banno, H. and Chua, N. (2000) Characterization of the arabidopsis formin-like protein AFH1 and its interacting protein. *Plant Cell Physiol.* **41**, 617–626.

Bolte, S., Talbot, C., Boutte, Y., Catrice, O., Read, N.D. and Satiat-Jeunemaitre, B. (2004) FM-dyes as experimental probes for dissecting vesicle trafficking in living plant cells. *J. Microscopy*, **214**, 159–173.

Bonifacino, J.S. and Traub, L.M. (2003) Signals for sorting of transmembrane proteins to endosomes and lysosomes. *Annu Rev. Biochemistry*, **72**, 395–447.

Burgess, J. and Northcote, D.H. (1968) The relationship between the endoplasmic reticulum and microtubular aggregation and disaggregation. *Planta*, **80**, 1–14.

Buschmann, H., Chan, J., Sanchez-Pulido, L., Andrade-Navarro, M.A., Doonan, J.H. and Lloyd, C.W. (2006) Microtubule-associated AIR9 recognizes the cortical division site at preprophase and cell-plate insertion. *Curr. Biol.* **16**, 1938–1943.

Cheung, A.Y. and Wu, H.M. (2004) Overexpression of an Arabidopsis formin stimulates supernumerary actin cable formation from pollen tube cell membrane. *Plant Cell*, **16**, 257–269.

Cleary, A.L. (1995) F-actin redistributions at the division site in living *Tradescantia* stomatal complexes as revealed by microinjection of rhodamine-phalloidin. *Protoplsama*, **185**, 152–165.

Cleary, A.L., Gunning, B.E.S., Wasteneys, G.O. and Hepler, P.K. (1992) Microtubule and F-actin dynamics at the division site in living *Tradescantia* stamen hair cells. *J. Cell Sci.* **103**, 977–988.

Cvrckova, F. (2000) Are plant formins integral membrane proteins? *Genome Biol.* **1**, 1–7.

Deeks, M.J., Hussey, P.J. and Davies, B. (2002) Formins: intermediates in signal-transduction cascades that affect cytoskeletal reorganization. *Trends Plant Sci.* **7**, 492–498.

Dhonukshe, P., Mathur, J., Hulskamp, M. and Gadella, T. (2005) Microtubule plus-ends reveal essential links between intracellular polarization and localized modulation of endocytosis during division-plane establishment in plant cells. *BMC Biology*, **3**, 11.

Dixit, R. and Cyr, R. (2002) Golgi secretion is not required for marking the preprophase band site in cultured tobacco cells. *Plant J.* **29**, 99–108.

Favery, B., Chelysheva, L.A., Lebris, M., Jammes, F., Marmagne, A., de Almeida-Engler, J., Lecomte, P., Vaury, C., Arkowitz, R.A. and Abad, P. (2004) Arabidopsis formin AtFH6 is a plasma membrane-associated protein upregulated in giant cells induced by parasitic nematodes. *Plant Cell*, **16**, 2529–2540.

Galatis, B. (1982) The organization of microtubules in guard cell mother cells of *Zea mays*. *Can. J. Bot.* **60**, 1148–1166.

Galatis, B. and Mitrakos, K. (1979) On the differential divisions and preprophase microtubule bands involved in the development of stomata of *Vigna sinensis* L. *J. Cell Sci.* **37**, 11–37.

Galatis, B., Apostolakos, P., Katsaros, C. and Loukari, H. (1982) Preprophase microtubule band and local wall thickening in guard cell mother cells of some Leguminosae. *Ann. Bot.* **50**, 779–791.

Gifford, M.L., Robertson, F.C., Soares, D.C. and Ingram, G.C. (2005) ARABIDOPSIS CRINKLY4 function, internalization, and turnover are dependent on the extracellular crinkly repeat domain. *Plant Cell*, **17**, 1154–1166.

Gunning, B.E.S. and Wick, S.M. (1985) Preprophase bands, phragmoplasts, and spatial control of cytokinesis. *J. Cell Sci.* (Suppl. 2), 157–179.

Gunning, B.E.S., Hardham, A.R. and Hughes, J.E. (1978) Pre-prophase bands of microtubules in all categories of formative and proliferative cell division in *Azolla* roots. *Planta*, **143**, 145–160.

Jürgens, G. (2004) Membrane trafficking in plants. *Annu. Rev. Cell Develop. Biol.* **20**, 481–504.

Kim, S.T., Zhang, K., Dong, J. and Lord, E.M. (2006) Exogenous free ubiquitin enhances lily pollen tube adhesion to an in vitro stylar matrix and may facilitate endocytosis of SCA. *Plant Physiol.* **142**, 1397–1411.

Kirchhausen, T. (2000) Clathrin. *Annu. Rev. Biochem.* **69**, 699–727.

Kremer, J.R., Mastronarde, D.N. and McIntosh, J.R. (1996) Computer visualization of three-dimensional image data using IMOD. *J. Structural Biol.* **116**, 71–76.

Liu, B. and Palevitz, B.A. (1992) Organization of cortical microfilaments in dividing root cells. *Cell Motil. Cytoskel.* **23**, 252–264.

Low, P.S. and Chandra, S. (1994) Endocytosis in plants. *Annu. Rev. Plant Physiol. Plant Mol. Biol.* **45**, 609–631.

Marcus, A.I., Dixit, R. and Cyr, R.J. (2005) Narrowing of the preprophase microtubule band is not required for cell division plane determination in plants. *Protoplasma*, **226**, 169–174.

Mineyuki, Y. (1999) The preprophase band of microtubules: Its function as a cytokinetic apparatus in higher plants. *Int. Rev. Cytol.* **187**, 1–49.

Mineyuki, Y. and Gunning, B.E.S. (1990) A role for preprophase bands of microtubules in maturation of new cell-walls, and a general proposal on the function of preprophase band sites in cell-division in higher-plants. *J. Cell Sci.* **97**, 527–537.

Mineyuki, Y. and Palevitz, B.A. (1990) Relationship between preprophase band organization, F-actin and the division site in *Allium*. Fluorescence and morphometric studies on cytochalasin-treated cells. *J. Cell Sci.* **97**, 283–295.

Mineyuki, Y., Wick, S.M. and Gunning, B.E.S. (1988) Preprophase bands of microtubules and the cell-cycle - kinetics and experimental uncoupling of their formation from the nuclear-cycle in onion root-tip cells. *Planta*, **174**, 518–526.

Mineyuki, Y., Marc, J. and Palevitz, B.A. (1989) Development of the preprophase band from random cytoplasmic microtubules in guard mother cells of *Allium cepa* L. *Planta*, **178**, 291–296.

Mineyuki, Y., Yamashita, M. and Nagahama, Y. (1991) p34^{cdc2} kinase homologue in the preprophase band. *Protoplasma*, **162**, 182–186.

Murata, T., Karahara, I., Kozuka, T., Giddings, T.H., Jr, Staehelin, L.A. and Mineyuki, Y. (2002) Improved method for visualizing coated pits, microfilaments, and microtubules in cryofixed and freeze-substituted plant cells. *J. Electron Microsc.* **51**, 133–136.

Nogami, A., Suzaki, T., Shigenaka, Y., Nagahama, Y. and Mineyuki, Y. (1996) Effects of cycloheximide on preprophase bands and prophase spindles in onion (*Allium cepa* L.) root tip cells. *Protoplasma*, **192**, 109–121.

Otegui, M.S., Mastronarde, D.N., Kang, B.H., Bednarek, S.Y. and Staehelin, L.A. (2001) Three-dimensional analysis of syncytial-type cell plates during endosperm cellularization visualized by high resolution electron tomography. *Plant Cell*, **13**, 2033–2051.

Packard, M.J. and Stack, S.M. (1976) The preprophase band: possible involvement in the formation of the cell wall. *J. Cell Sci.* **22**, 403–411.

Pickett-Heaps, J.D. (1974) Plant microtubules. In *Dynamic Aspects of Plant Ultrastructure* (Robards, A.W., ed). London: McGraw Hill, pp. 219–255.

Pickett-Heaps, J.D. and Northcote, D.H. (1966a) Organization of microtubules and endoplasmic reticulum during mitosis and cytokinesis in wheat meristems. *J. Cell Sci.* **1**, 109–120.

Pickett-Heaps, J.D. and Northcote, D.H. (1966b) Cell division in the formation of the stomatal complex of the young leaves of wheat. *J. Cell Sci.* **1**, 121–128.

Russinova, E., Borst, J.W., Kwaaitaal, M., Cano-Delgado, A., Yin, Y., Chory, J. and De Vries, S.C. (2004) Heterodimerization and endocytosis of Arabidopsis brassinosteroid receptors BRI1 and AtSERK3 (BAK1). *Plant Cell*, **16**, 3216–3229.

Seguí-Simarro, J.M. and Staehelin, L.A. (2006) Cell cycle-dependent changes in Golgi stacks, vacuoles, clathrin-coated vesicles and multivesicular bodies in meristematic cells of *Arabidopsis thaliana*: a quantitative and spatial analysis. *Planta*, **223**, 223–236.

Seguí-Simarro, J.M., Austin, J.R., II, White, E.A. and Staehelin, L.A. (2004) Electron tomographic analysis of somatic cell plate formation in meristematic cells of arabidopsis preserved by high-pressure freezing. *Plant Cell*, **16**, 836–856.

Shah, K., Russinova, E., Gadella, T.W.J., Willemse, J. and de Vries, S.C. (2002) The *Arabidopsis* kinase-associated protein phosphatase controls internalization of the somatic embryogenesis receptor kinase 1. *Genes Dev.* **16**, 1707–1720.

Sinnott, E.W. (1960) *Plant Morphogenesis*. New York: McGraw-Hill.

Smith, L.G., Hake, S. and Sylvester, A.W. (1996) The *tangled1* mutation alters cell division orientations throughout maize leaf development without altering leaf shape. *Development*, **122**, 481–489.

Staehelin, L.A. and Chapman, R.L. (1987) Secretion and membrane recycling in plant cells: novel intermediary structures visualized in ultrarapidly frozen sycamore and carrot suspension-culture cells. *Planta*, **171**, 43–57.

Tahara, H., Yokota, E., Igarashi, H., Orii, H., Yao, H., Sonobe, S., Hashimoto, T., Hussey, P.J. and Shimmen, T. (2007) Clathrin is involved in organization of mitotic spindle and phragmoplast as well as in endocytosis in tobacco cell cultures. *Protoplasma*, **230**, 1–11.

Tse, Y.C., Mo, B., Hillmer, S., Zhao, M., Lo, S.W., Robinson, D.G. and Jiang, L. (2004) Identification of multivesicular bodies as prevacuolar compartments in *Nicotiana tabacum* BY-2 cells. *Plant Cell*, **16**, 672–693.

Van Damme, D., Coutuer, S., De Rycke, R., Bouget, F.Y., Inzé, D. and Geelen, D. (2006) Somatic cytokinesis and pollen maturation in Arabidopsis depend on TPLATE, which has domains similar to coat proteins. *Plant Cell*, **18**, 3502–3518.

Vanstraelen, M., Van Damme, D., De Rycke, R., Mylle, E., Inzé, D. and Geelen, D. (2006) Cell cycle-dependent targeting of a kinesin at the plasma membrane demarcates the division site in plant cells. *Curr. Biol.* **16**, 308–314.

Walker, K.L., Muller, S., Moss, D., Ehrhardt, D.W. and Smith, L.G. (2007) *Arabidopsis* TANGLED identifies the division plane throughout mitosis and cytokinesis. *Curr. Biol.* **17**, 1827–1836.

Wick, S.M. and Duniec, J. (1983) Immunofluorescence microscopy of tubulin and microtubule arrays in plant cells. I. Pre-prophase band development and concomitant appearance of nuclear envelope-associated tubulin. *J. Cell Biol.* **97**, 235–243.

Wick, S.M., Seagull, R.W., Osborn, M., Weber, K. and Gunning, B.E.S. (1981) Immunofluorescence microscopy of organized microtubule arrays in structurally stabilized meristematic plant cells. *J. Cell Biol.* **89**, 685–690.